Research article

Phenotypic alterations in articulating joint cells: Role of mechanically loaded MSC secretome

Yann D. Ladner [a,b], Ursula Menzel [a], Keith Thompson [c], Angela R. Armiento [c], Martin J. Stoddart [a,d,*]

[a] AO Research Institute Davos, Clavadelerstrasse 8, 7270, Davos Platz, Switzerland
[b] Institute for Biomechanics, ETH Zurich, Lengghalde 5, CH-8008, Zurich, Switzerland
[c] UCB Pharma, Slough, UK
[d] Department of Orthopedics and Trauma Surgery, Medical Center-Albert-Ludwigs-University of Freiburg, Faculty of Medicine, Albert-Ludwigs-University of Freiburg, 79106, Freiburg, Germany

ABSTRACT

Improvements in the treatment of cartilage require insights into the secretory profile of mesenchymal stem cells (MSCs). Apart from their differentiation potential, MSCs secrete a multitude of molecules with therapeutic properties that benefit chondrogenesis and immunomodulation. Previously, we employed a small-panel microarray to demonstrate differences within conditioned medium (CM) of MSCs that were mechanically stimulated within a joint-mimicking bioreactor and their unloaded controls.

This study analyzed the proteomic content within CM from 4 week mechanically loaded MSCs with a larger protein microarray. We examined the chondrogenic effect of CM by administration to MSC and chondrocyte pellet cultures, as well as functional changes in T cell proliferation.

CM from mechanically loaded samples shows a promising push towards chondrogenic phenotypes within both pellet cultures. Inhibition of T cell proliferation was also observed. This *in vitro* model could enhance our understanding how mechanical load induces changes in MSC secretome benefitting cartilage healing.

1. Introduction

Articular cartilage (AC) is the tissue withstanding the loads within an articulating joint. It lines the surface between bones and minimizes compressive and shear forces. However, due to the lack of blood vessels and the low metabolic activity of the sparsely embedded cells, cartilage lesions can lead to post-traumatic osteoarthritis (PTOA). PTOA is a major musculoskeletal disorder that accounts for 12 % of cases with osteoarthritis (OA), resulting in massive health-care costs [1,2].

Current cartilage-restoring strategies can be divided into surgical-only, regenerative medicine and tissue engineering approaches [3]. Surgical-only techniques include marrow stimulation procedures such as microfracture (MFx), where small defects are made into the subchondral bone, allowing the formation of a blood clot that contains bone marrow stem/stromal cells. These cells are assumed to be directed towards chondrogenesis for the replacement of the lost cartilage [4]. Regenerative medicine approaches such as autologous chondrocyte implantation (ACI) involve implanting the patient's own cartilage cells from a healthy, non-weight-bearing site to the

---

injured site. Before implantation, the cartilage cells require *in vitro* expansion, as they are low in number. Lastly, tissue engineering procedures combine cells, scaffolds, biochemical and physical stimuli *in vitro* to regenerate the tissue, which is then implanted [5].

However, these approaches are hampered by shortcomings: amongst others, MFx results in mechanically inferior fibrocartilage [6], ACI involves two invasive procedures and cartilage cells dedifferentiate during their expansion [7], while the use of MSCs for cartilage tissue engineering requires a large number of cells [8].

Naturally, insights from one approach can be used for the other approaches. For example, *in vitro* tissue engineering models could explain why microfracture leads to mechanically inferior fibrocartilage [9]. On the other hand, microfracture can be extended through tissue engineering concepts by use of a collagen matrix to stabilize the blood clot in a procedure termed autologous matrix-induced chondrogenesis (AMIC) [10].

Notably, our group developed a model that loosely represents the environment after AMIC [11]. Mesenchymal stem/stromal cells (MSCs) are encapsulated in fibrin that emulates the blood clot containing the bone marrow elements and then seeded into a porous polyurethane scaffold. The polyurethane sponge reinforces the 3D structure to withstand the unconfined, joint-mimicking compressive and shear loads exerted by a bioreactor. Simultaneously, the scaffold is sufficiently elastomeric to allow for repeated loading. By exposing the MSCs to these stimuli, mechanical activation of transforming growth factor β1 (TGF-β1) was demonstrated [12–14]. TGF-β1 is a key player in chondrogenesis and usually secreted in an inactive form by MSCs [15]. While investigating further effects of the mechanical loading, it became apparent that other proteins were differentially secreted between loaded and unloaded scaffolds. Amongst others, there were factors that play a role in angiogenesis, hypertrophy and immunomodulation, such as angiopoietin-2, growth related oncogene α and nitric oxide (NO) [16].

The plethora of secreted factors is termed secretome and includes soluble proteins, lipids, extracellular vesicles and micro-RNAs [17–20]. Investigating the secretory profile of MSCs could elicit how the cells exert their therapeutic potential. In fact, a study by de Windt et al. showed the regenerative effect of MSCs on cartilage even though the cells could not be detected after a 12-month period [21]. This suggests that MSCs might affect target cells either via their secretome or direct cell-to-cell contacts. Furthermore, using only the MSC secretome as opposed to cell delivery would benefit clinical translation with its longer shelf-life and a superior safety profile [22,23]. Another study investigated *in vitro* co-culture of MSCs with chondrocytes (Cho) within their pericellular matrix and found that MSCs enhanced matrix preservation and synthesis [24]. Evidently, more work is needed to establish the role of the different factors and their therapeutic effect.

In the present work, we exposed MSCs to joint-mimicking multi-axial load within a custom bioreactor (described in Ref. [25]) and harvested the conditioned medium (CM) to analyze the soluble protein fraction of the secretome. Thereafter, we investigated the effect of CM on two chondrogenic models, namely on MSC and Cho pellets. As the CM could also affect cartilage adjacent tissue, such as synovium, we presented the CM to immune cells. Notably, T cells have been shown to be implicated in OA, by recruiting macrophages and directly degrading cartilage [26]. We therefore also conducted an experiment to observe the effect of mechanical stimulation on the immunosuppressive properties of MSC secretome. The aim of the study was to assess the effect of mechanically stimulated MSC secretome on cell phenotype, with an additional group containing TGF-β included as a control. As we have previously shown that classical chondrogenic media containing 10 ng/mL TGF-β obscures any effect of loading [14], we chose a more physiological dose of 2 ng/mL to assess whether there was any modulation of the response to load.

2. Materials and methods

2.1. Isolation, culture and seeding of MSCs

Human MSCs were isolated with full ethical approval (Freiburg, EK-326/08) and written informed donor consent from bone marrow aspirates of 9 donors using Ficoll (Histopaque®-1077, Sigma-Aldrich) density gradient and plastic adhesion [27].

6 donors were used for scaffold seeding and later the mechanical stimulation experiment with the goal to produce CM (four females aged 18, 48, 51, 57; 2 males aged 18, 55). 3 donors were used for a pellet experiment (two males aged 30 and 53; one female aged 55).

After isolation, MSCs were expanded in Minimum Essential Medium alpha (αMEM, Gibco) supplemented with 10 % (v/v) fetal bovine serum (FBS, Corning), 1 % (v/v) Penicillin-Streptomycin (P/S, 100 U/mL penicillin and 100 µg/mL streptomycin, Gibco) and 5 ng/mL recombinant human fibroblast growth factor basic protein (FGF-b, Fitzgerald Industries International). The cells were cultured until passage 4 before scaffold seeding and until passage 3 before pellet formation before seeding into scaffolds, as described previously [12,28]. Briefly, 4.5×10^6 cells were seeded into a cylindrical fibrin-poly(ester-urethane) (fibrin-PU) scaffold (average salt leached pore size between 150 and 300 µm) with a thickness of 4 mm and a diameter of 8 mm according to previous protocols [12,28]. The cells were resuspended in 50 mg/mL fibrinogen (Sigma-Aldrich) and added to the sterile lid of a 1.5-mL Eppendorf tube. An equal volume of a 4 U/mL thrombin solution (Sigma-Aldrich) was then mixed with the fibrinogen-cell solution and the porous scaffold was pressed into the lid. Repeated compression of the scaffold using tweezers allowed for the influx of the cell suspension into the pores and even cell distribution as previously shown [11]. Afterwards, the scaffolds were transferred to a cell culture incubator (37 °C, 5 % CO_2 and 95 % rH) for 40 min. Another 0.5×10^6 cells were suspended in Dulbecco's modified Eagle medium 4.5 g/L glucose (DMEM, Gibco) and seeded on top of the scaffolds with subsequent incubation for 1 h, to mimic a superficial layer as originally described by Gardner et al. [12]. Thereafter, the scaffolds were placed into polyether ether ketone (PEEK) sample holders that allowed for mechanical stimulation and then into the bioreactor within a cell culture incubator. Unloaded control samples were transferred to similar PEEK sample holders and kept in 100 mm Petri dishes within the same incubator as the bioreactor. All scaffold samples were cultured in chondropermissive medium (CpM) consisting of 4.5 g/L DMEM, 0.11 g/L sodium pyruvate (Sigma-Aldrich), 50 µg/mL L-ascorbic acid 2-phosphate ses-quimagnesium salt hydrate (Sigma-Aldrich), 100 nM dexamethasone (Sigma-Aldrich), Corning™ ITS + Premix (6.25 µg/mL human

recombinant insulin, 6.25 μg/mL human natural transferrin, 6.25 ng/mL selenious acid, 1.25 mg/mL bovine serum albumin, 5.35 μg/mL linoleic acid, ThermoFisher), 1 % non-essential amino acids (Gibco), 1 % (v/v) Penicillin/Streptomycin (P/S) and 5 μM 6-aminocaproic acid (Sigma-Aldrich). In contrast to the chondrogenic medium that is commonly found in literature, the chondropermissive medium consists of the same reagents except for the growth factor TGF-β. This enables the investigation whether other factors, such as mechanical loading, exert a similar chondrogenic effect as exogenously added TGF-β1. The culture conditions were kept constant at 37 °C, 5 % CO_2 and 95 % rH.

2.2. Mechanical loading, production of conditioned medium and scaffold harvest

For the mechanical loading experiment, MSCs from 6 donors within scaffolds (section 3) were exposed to multi-axial load within a custom-made multi-well bioreactor (MWB), 24 h after seeding, as described previously [25]. Both unloaded (UL) and loaded samples (L) – within the MWB – were kept in the same standard incubator. The loading protocol consisted of a cyclical back-and-forth motion of a teardrop-shaped counterface at 1 Hz. The shape introduces a combination of compression and shear. Namely, 10 % pre-strain is superimposed on 20 % dynamic strain, resulting in a strain range of 10–30 % compression. This loading protocol was run twice per day (morning and afternoon) for 1 h each, twice a day for 28 consecutive days. Unloaded controls were kept in free-swelling conditions within the same incubator. Medium was replaced 3 times per week. Once harvested, the CM was first centrifuged at 13′000 relative centrifugal force (RCF) and then stored at −20 °C for later analysis. At the end of the experiment (after 28 days), the scaffolds were digested in 1 mL 0.5 mg/mL proteinase K (pK, Roche) at 56 °C for 16 h. The pK reaction was inactivated at 96 °C for 10 min and the samples were stored at −20 °C.

2.3. Isolation and culture of Cho

Human osteoarthritic chondrocytes (Cho) were isolated from femoral heads of 3 patients (two females aged 71 and 74; one male aged 83) who underwent hip replacement operation with their informed consent and approval by the cantonal ethical commission (KEK-ZH-NR: 2010-0444/0) using the protocol of Francioli et al. [29].

After isolation, Cho were cultured in base medium of 4.5 g/L glucose DMEM, 10 % FBS, 1 % (v/v) P/S, 0.11 g/L sodium pyruvate, 1 % non-essential amino acids, 100 mmol/L of HEPES buffer solution (Gibco) and 0.29 mg/mL of L-Glutamine (Gibco). For the expansion up to passage 3, the base medium was supplemented with 1 ng/mL TGF-β1 (Fitzgerald Industries International) and 5 ng/mL FGF- β. Standard culture conditions were employed (37 °C, 5 % CO_2 and 95 % rH).

2.4. Protein microarray

The CM acquired during the loading experiment was pooled by week 2, 3 and 4 and load type (load type: loaded (L) and the unloaded controls (UL)). As an example, ULw2 (CM from UL samples of week 2) consists of medium from the unloaded scaffolds of all 6 donors during week 2. Additionally, a reference sample was kept consisting of CM that was exposed to the cells within the scaffolds for one day before any loading stimulus (day0) and a cell-free CpM sample was used for background subtraction. Together, this resulted in the following test samples:

- ULw2 (**UnL**oaded **w**eek **2**)
- ULw3
- ULw4
- Lw2 (**L**oaded **w**eek **2**)
- Lw3
- Lw4
- Day0
- CpM

The proteins within the pooled conditioned media were then detected using a Human L2000 glass slide array (RayBiotech) according to manufacturer's instructions. The signal intensities of the positive controls on the array were used to normalize the results. In

Table 1
Treatment media for MSC and Cho pellet experiment.

Condition	Name of condition	Base medium	Refreshment medium	TGF-β1 (ng/mL)
1	CpM-	CpM	CpM	0
2	CpM+	CpM	CpM	2
3	UL CM-	UL CM	CpM	0
4	UL CM+	UL CM	CpM	2
5	L CM-	L CM	CpM	0
6	L CM+	L CM	CpM	2

CpM: chondropermissive medium; CM: conditioned medium; UL: unloaded; L: loaded.

addition, the intensities obtained from the CpM (acting as blank) were subtracted from the intensities of the test samples.

An interactive Shiny [30] application visualizing all the values can be found under:
https://yannladner.shinyapps.io/TAC-Analysis/?_inputs_&tabs="targets_RB"

2.5. Pellet experiments with MSCs and Cho

Two pellet experiments were performed: one with 3 MSC donors, another with 3 Cho donors. For both experiments, cells were trypsinized at passage 3 and 200 μL aliquots of 2×10^5 cells in CpM were centrifuged at 500 RCF for 5 min in V-bottom 96-well plates (ThermoFisher) [27]. The plates were transferred to an incubator to allow pellet formation. Thereafter, the medium was replaced with 200 μL of treatment culture media. Table 1 shows the conditions for the MSC pellet and Cho pellet experiments. For both cell culture types, there were 6 conditions. The three base medium conditions, namely chondropermissive medium (CpM), conditioned medium from unloaded scaffolds (UL CM) and conditioned medium from loaded scaffolds (L CM) were supplemented in a ratio of 1:1 (as seen in Table 1: Part A:Part B) with the refreshment medium CpM. The base media containing CM consisted of CM pooled from weeks 2–4. All three base medium conditions were then either supplemented with 2 ng/mL TGF-β1 (denoted with a "+", *e.g.* CpM+) or without TGF-β1 (denoted with a "-", *e.g.* CpM-). 2 ng/mL of TGF-β1 instead of the usual 10 ng/mL were chosen as not to obfuscate a possible synergetic effect of CM and TGF-β1. The culture conditions were kept constant at 37 °C, 5 % CO_2 and 95 % rH. MSC and Cho pellets were cultured for 28 days and 21 days, respectively.

2.6. T cell proliferation

Ethical approval was granted by the cantonal ethical committee of Grisons (BASEC-Nr. 2019–02353). The blood from 3 healthy donors was collected by venous puncture and transferred into potassium EDTA-coated tubes (S-Monovette®, Sarstedt). Peripheral blood mononuclear cells (PBMCs) were isolated using Ficoll density gradient separation (Histopaque®-1077, Sigma-Aldrich).

PBMCs were kept in RPMI 1640 (Gibco) containing 2 mM L-glutamine, supplemented with 10 % (v/v) heat inactivated fetal calf serum (Biochrom), 1 % (v/v) Penicillin-Streptomycin (P/S, 100 U/mL penicillin and 100 μg/mL streptomycin, Gibco), 30 U/mL interleukin 2 (IL-2, PeproTech). Standard culture conditions were employed (37 °C, 5 % CO_2 and 95 % rH).

For the proliferation experiment, PBMCs were stained with 3 μM PKH26 (Sigma-Aldrich) and transferred to 48-well plates at 500′000 cells per well. 5×10^6 Human T-Activator Dynabeads® (Gibco) per well were used for the proliferation. The different experimental conditions consisted of CM from unloaded (UL_w2) and loaded (L_w2) scaffolds from week 2 that were diluted 1:1 in the above-mentioned culture medium. Afterwards, the CM were either depleted (via immunoprecipitation) of TGF-β with a TGF-β1, 2, 3 antibody (R&D Systems) or with a Mouse IgG1 Isotype antibody (R&D Systems) as a control to determine the effect of TGF-β on T cell proliferation. The medium was refreshed with 30 U/mL IL-2 after 3 days and T cell proliferation was measured after 4 days using the FACSAria III Cell Sorter (BD). Raw data was analyzed to calculate a division index using the "Proliferation platform" within FlowJo 10.4 (FlowJo LLC) [31]. The division index corresponds to the number of cells at the start of culture divided by the total number of divisions.

2.7. Biochemical assays

Hoechst 33258 dye (Sigma) was used to quantify the DNA content by measuring fluorescence at an excitation at 355 nm and emission at 460 nm. The 1,9-dimethylmethylene blue (DMMB) assay was used to quantify the sulphated glycosaminoglycan (sGAG) content in the CM and pK digested samples. As described previously, absorbance was measured at 530 nm and the highest sGAG standard in the wells contained 1.25 μg to achieve a stable and linear standard curve [32]. The DNA content was used to normalize the sGAG content (within scaffolds, pellets or the CM), resulting in sGAG/DNA ratios. A DuoSet® ELISA kit (R&D Systems) was used to quantify TGF-β1 protein in the CM according to manufacturer's instructions. Absorbances were measured 450 nm and 560 nm, the values obtained at 560 nm subtracted from the values obtained at 450 nm, and the concentrations calculated by fitting a four-parameter logistic curve. Total produced TGF-β1 was measured by activation through acidification of the samples, prior to sample addition to the plate. Consequently, the total produced TGF-β1 consists of already active and activated TGF-β1. The different biochemical assays were measured using an Infinite® 200 PRO (Tecan) plate reader.

2.8. Gene expression

For RNA analysis, 2 pellets per group were transferred to 1 mL TRI reagent +5 μL Polyacryl Carrier (both Molecular Research Centre Inc., Cincinnati, OH, USA) and 5 mm metal balls (MARTIN & C) within 2-mL Eppendorf Safe-Lock® Tubes (Eppendorf). The samples were then homogenized in the TissueLyser II (Qiagen) for 2×3 min at 30 Hz. All steps were conducted at room temperature. After homogenization, the samples were centrifuged at 12′000 RCF at 4 °C to obtain the supernatant, which was transferred to a new 2-mL Eppendorf tube for subsequent RNA isolation according to Sigma's TRI Reagent® Protocol [33].

After isolation, the RNA was reverse transcribed using the SuperScript™ VILO™ cDNA Synthesis Kit (Invitrogen™). qRT-PCR within the QuantStudio™ 6 Pro Real-Time PCR System (ThermoFisher) was used to quantify the gene expression levels of collagens type I *(COL1A1)*, type II *(COL2A1)*, type X *(COL10A1)*, aggrecan *(ACAN)*, runt-related transcription factor 2 *(RUNX2)*, SRY-box transcription factor *(SOX9)*, Matrix metalloproteinase 3 and 13 *(MMP3, MMP13)*, Mitochondrially encoded cytochrome C oxidase II *(COX2)*, interleukin 6, 8, and 10 *(IL6, IL8, IL10)*, tumor necrosis factor *(TNF)*, and versican *(VCAN)* and ribosomal protein lateral stalk

subunit P0 *(RPLP0)*.

Primers and probes for qRT-PCR are listed in Table 2. The gene expression was analyzed using the $2^{-\Delta\Delta CT}$ method [34] with *RPLP0* as housekeeping gene and relative to day 0 (1 day after seeding and before the first loading). *COL1A1* was chosen as a marker of fibrocartilage, *COL2A1, ACAN, SOX9* and *VCAN* for chondrogenesis, *COL10A1, MMP3, MMP13* and *RUNX2* for hypertrophy, *COX2, IL6, IL8, IL10* and *TNF* for inflammation.

2.9. Pellet area quantification

Brightfield images of the pellets within the well plates were taken using a ZEISS Axio Vert.A1 microscope using AxioVision software (Carl Zeiss). Paint.net (dotPDN, LLC) was used to crop the pellets for later area quantification using ImageJ [35].

2.10. Histology

Pellets were fixed with 10 % (v/v) neutral buffered Formalin solution (Sigma-Aldrich) at room temperature for 24 h, then transferred to 70 % (v/v) ethanol at 4 °C. To prevent loss of pellets during the embedding the pellets were embedded in 2 % (w/v) wide range agarose (Sigma-Aldrich) and subsequently processed for embedding in paraffin according to routine protocol. Samples were sectioned at a thickness of 5 μm. After deparaffinization using xylene and subsequent hydration, sections were stained with Safranin O/ Fast Green (both Sigma) and counterstained with Weigert's haematoxylin (Merck) following routine protocol.

2.11. Statistical analysis

All statistical analyses and visualizations were conducted using R (4.3.0) within RStudio (2023.6.0.421) [36,37]

To analyze the protein microarray data using principal component analysis (PCA), the obtained values were centered and scaled by the proteins' respective standard deviations. The R package *PCAtools* was used to conduct the PCA [38]. The Venn diagram was visualized using *ggvenn* [39].

Significance Analysis of Microarrays (SAM) was employed using the R package *samr* [40]. After centering the microarray data by the median, a two-class paired model was used for the weekly pooled targets (ULw2 vs. Lw2, ULw3 vs. Lw3, ULw4 vs. Lw4), with a minimum fold change of 2 and the α for the false discovery rate set to 0.05.

For the analysis of the pellet experiments, linear mixed models were employed with donor as random effect. Estimated marginal means were adjusted using the Tukey method. For the linear mixed model, the R packages *lmer* and *lmerTest* were used and for the estimated marginal means, the R package *emmeans* was used [41–43]. This allows analysis of data sets where some genes are not detected. Error bars show standard error of mean (SEM).

3. Results

3.1. Mechanical loads increases DNA content

The DNA ratio, consisting of the DNA content of day 28 over day 0 samples, was significantly higher for loaded scaffolds (L) compared to their unloaded controls (UL) (UL: 0.67 ± 0.02; L: 0.91 ± 0.04 – Fig. 1).

Table 2
Primers and probe sequences for qRT-PCR.

Gene	Forward primer	Reverse primer	Probe
ACAN	5′-AGT CCT CAA GCC TCC TGT ACT CA-3′	5′-CGG GAA GTG GCG GTA ACA-3′	5′-CCG GAA TGG AAA CGT GAA TCA GAA TCA ACT-3′
COL1A1	5′-CCC TGG AAA GAA TGG AGA TGA T-3′	5′-ACT GAA ACC TCT GTG TCC CTT CA-3′	5′-CGG GCA ATC CTC GAG CAC CCT -3′
COL2A1	5′-GGC AAT AGC AGG TTC ACG TAC A-3′	5′-GAT AAC AGT CTT GCC CCA CTT ACC-3′	5′-CCT GAA GGA TGG CTG CAC GAA ACA TAC-3′
COL10A1	5′-ACG CTG AAC GAT ACC AAA TG-3′	5′-TGC TAT ACC TTT ACT CTT TAT GGT GTA-3′	5′-ACT ACC CAA CAC CAA GAC ACA GTT CTT CAT TCC-3′
COX2	5′-TTG TAC CCG GAC AGG ATT CTA TG-3′	5′-TGT TTG GAG TGG GTT TCA GAA ATA-3′	5′-GAA AAC TGC TCA ACA CCG GAA TTT TTG ACA A-3′
IL6	Assay ID[a]: Hs00174131_m1		
IL8	Assay ID[a]: Hs00174103_m1		
IL10	Assay ID[a]: Hs00961622_m1		
MMP3	Assay ID[a]: Hs00968305_m1		
MMP13	5′-CGG CCA CTC CTT AGG TCT TG-3′	5′-TTT TGC CGG TGT AGG TGT AGA TAG-3′	5′-CTC CAA GGA CCC TGG AGC ACT CAT GT-3′
RPLP0	5′-TGG GCA AGA ACA CCA TGA TG-3′	5′-CGG ATA TGA GGC AGC AGT TTC-3′	5′-AGG GCA CCT GGA AAA CAA CCC AGC-3′
RUNX2	5′-AGC AAG GTT CAA CGA TCT GAG AT-3′	5′-TTT GTG AAG ACG GTT ATG GTC AA-3′	5′-TGA AAC TCT TGC CTC GTC CAC TCC G-3′
VCAN	Assay ID[a]: Hs00171642_m1		

[a] TaqMan™ Gene Expression Assay.

3.2. sGAG content within scaffolds is increased, yet lower within CM of unloaded controls

After 28 days, L scaffolds retained significantly more sGAG than UL (UL: 3.71 µg/µg±0.09; L: 22.22 µg/µg±2.01 – $p < .0001$). Additionally, more sGAG was detected in L scaffolds with time (UL day 0: 1.81 µg/µg±0.06 – Fig. 2A).

Conversely, the sGAG content within pooled CM was significantly higher in UL than in L for both weeks 2 and 4 (Week 2: UL: 9.23 µg/µg±0.64; L: 5.12 µg/µg±0.17, $p < .01$, Week 4 UL: 8.82 µg/µg±0.42; L: 5.33 µg/µg±0.34, $p < .01$ – Fig. 2B).

3.3. Protein profile within the CM shows differences within loaded and unloaded samples

97.2 % of the proteins on the 2000 protein microarray were found in the CM of both L and UL samples (Fig. 3). 1.3 % and 1.5 % of all proteins were found only in L and UL samples, respectively (Fig. 3A). Principal component (PC) 1, which accounted for 56.08 % of the variation, discriminated between CM from UL and L samples. PC2, which accounted for 27.72 % of the variation, discriminated between CM of d0 samples and samples that were loaded for 2–4 weeks.

Significance analysis of microarray (SAM) revealed 59 targets with higher expression levels for L CM than UL CM and 120 targets with higher expression levels for UL CM than L CM.

The complete list can be found in Supplementary Tables 7–1.

Furthermore, selected candidate targets (selection was based on previous study or significance and relevance to this study) are depicted in Supplementary Fig. 1 and an interactive Shiny app to visualize the entire results can be explored on the following webpage: https://yannladner.shinyapps.io/TAC-Analysis/?_inputs_&tabs="targets_RB"

3.4. Mechanical load activates TGF-β1

As expected, active TGF-β1 was only detected in L CM (Supplementary Fig. 2). Additionally, total produced TGF-β1 (latent and active) was higher in L CM compared to UL CM for both weeks 2 and 4.

3.5. Effect of CM on pellet area and DNA of MSC and Cho pellets

On day 28, MSC pellets exhibited a significantly smaller area when exposed to CM- (L and UL) compared to CpM- (CpM-: 1.03 mm^2 ± 0.1; UL CM-: 0.61 mm^2 ± 0.08; L CM: 0.77 mm^2 ± 0.12 – CpM-vs. UL CM-: $p < .0001$, CpM-vs. L CM-: $p < .01$ – Fig. 4A). TGF-β1 supplemented pellets show overall a larger area compared to pellets cultured without TGF-β1 ($p < .0001$). Similar to TGF-β1 free conditions, the area of MSC pellets was also significantly smaller when exposed to CM + compared to CpM+ (CpM+: 2.51 mm^2 ± 0.12; UL CM+: 1.5 mm^2 ± 0.19; L CM+: 1.81 mm^2 ± 0.11 – CpM-vs. UL CM-: $p < .0001$, CpM-vs. L CM-: $p < .0001$ – Fig. 4B).

In the absence of TGF-β, the DNA content of MSC pellets remained stable among the different conditions (Fig. 4B). When supplemented with 2 ng/mL TGF-β1, CpM + samples demonstrated the highest DNA content over all time points. Addition of conditioned medium to 2 ng/mL TGF-β1 containing samples led to a significant decrease in DNA content for day 7 (CpM+: 0.75 µg ± 0.1; UL CM+: 0.53 µg ± 0.08; L CM+: 0.58 µg ± 0.09 – CpM-vs. UL CM-: $p < .05$, CpM-vs. L CM-: $p < .05$).

Cho pellets exhibited a larger area for L CM-compared to both UL CM- and CpM- (CpM-: 2.52 mm^2 ± 0.09; UL CM-: 2.64 mm^2 ± 0.11; L CM-: 3.24 mm^2 ± 0.12 – CpM-vs. L CM-: $p < .0001$, UL CM-vs. L CM-: $p < .0001$ – Fig. 5A). A similar trend, albeit insignificant, was apparent for pellets exposed to 2 ng/mL TGF-β1.

Cho pellets demonstrated the highest DNA content when treated with L CM+ (Fig. 5B). A significant difference was apparent at day 7 between CpM+ and L CM+ (CpM+: 1.38 µg ± 0.05; L CM+: 1.75 µg ± 0.16 – CpM-vs. L CM-: $p < .05$) and at day 21 between CpM+ and L CM+ and UL CM+ and L CM+ (CpM+: 1.33 µg ± 0.08; UL CM+: 1.52 µg ± 0.12; L CM+: 1.74 µg ± 0.08, CpM+ – CpM + vs. UL CM+: $p < .01$, CpM + vs. L CM+: $p < .05$).
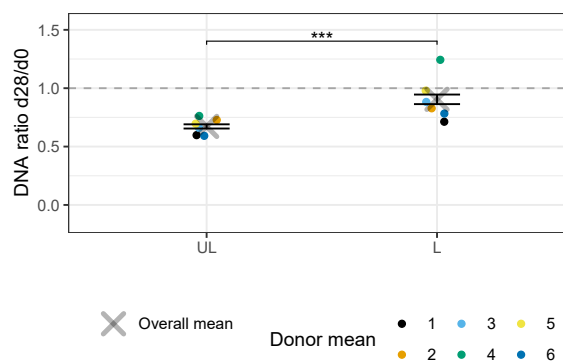

Fig. 1. DNA ratio (day 28 vs. day 0) of unloaded (UL) and loaded (L) scaffolds. Dashed line indicates a ratio of 1, which constitutes no change in DNA content between day 28 and day 0. Data from 6 donors. Error bars show SEM. ***$p < .001$.
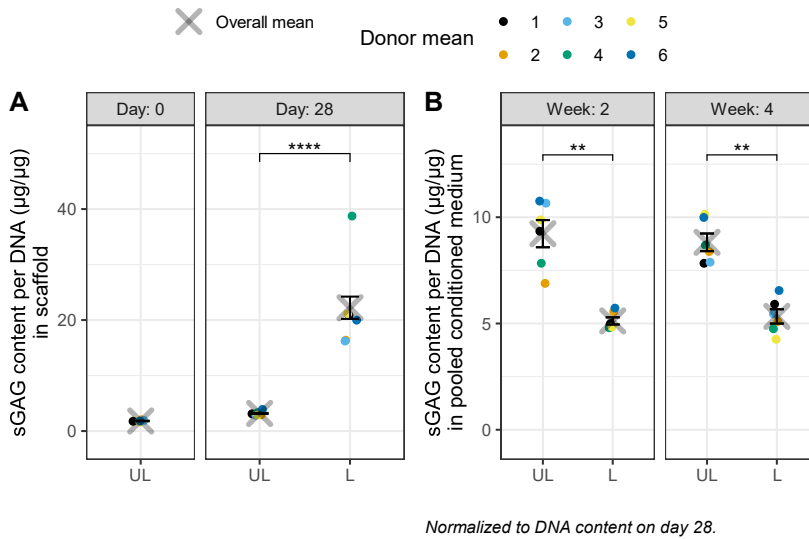
Fig. 2. sGAG content in sample and conditioned medium of unloaded (UL) and loaded (L) scaffolds. (A) sGAG content in day 0 and day 28 samples normalized to their DNA content. (B) sGAG content secreted into conditioned medium during week 2 and week 4 normalized to the DNA of respective samples. Conditioned medium from the same donors was pooled by week. Data from 6 donors. Error bars show SEM. **$p < .01$, ****$p < .0001$.
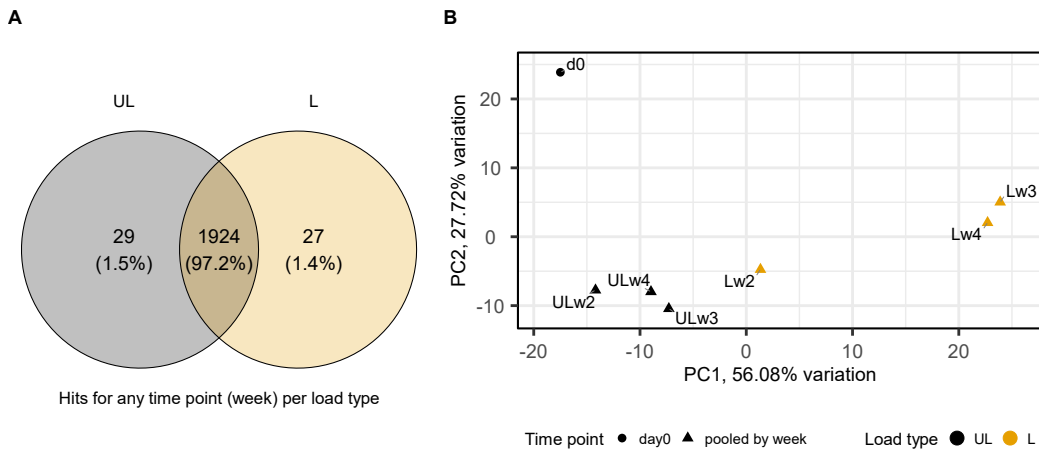

Fig. 3. Overview of protein microarray data. (A) Venn diagram of proteins detected in conditioned medium in unloaded (UL) and loaded (L) samples using the protein array. (B) Principal component analysis of conditioned medium from UL and L samples. W = week (*e.g.* Ulw3: unloaded sample from week 3). D0 refers to conditioned medium 24 h after seeding the cells into scaffolds. For each condition, samples were pooled from 6 donors by week for week 2, 3 and 4.

3.6. Effect of CM on sGAG content of pellets

By day 28, addition of 2 ng/mL TGF-β1 lead to an increased sGAG retention compared with CPM pellets at the same time point ($p <$ .05). In two out of three donors, L CM led to an increased sGAG/DNA compared to CpM by day 28, however this did not reach significance (Fig. 6). The combination of L CM and 2 ng/mL TGF-β1 led to a decrease in sGAG content within MSC pellets after 7 days (CpM+: 6.69 μg/μg±1.08; L CM+: 4.45 μg/μg±0.98 – CpM + vs. L CM+: $p <$ .05). This decrease was also apparent on day 28, without reaching significance. Longer exposure to TGF-β1 supplementation led to higher sGAG retention in all conditions.

Total sGAG content found in the CM of MSCs pellets was significantly higher for UL CM and L CM compared with CPM, with and without TGF-β1 addition.
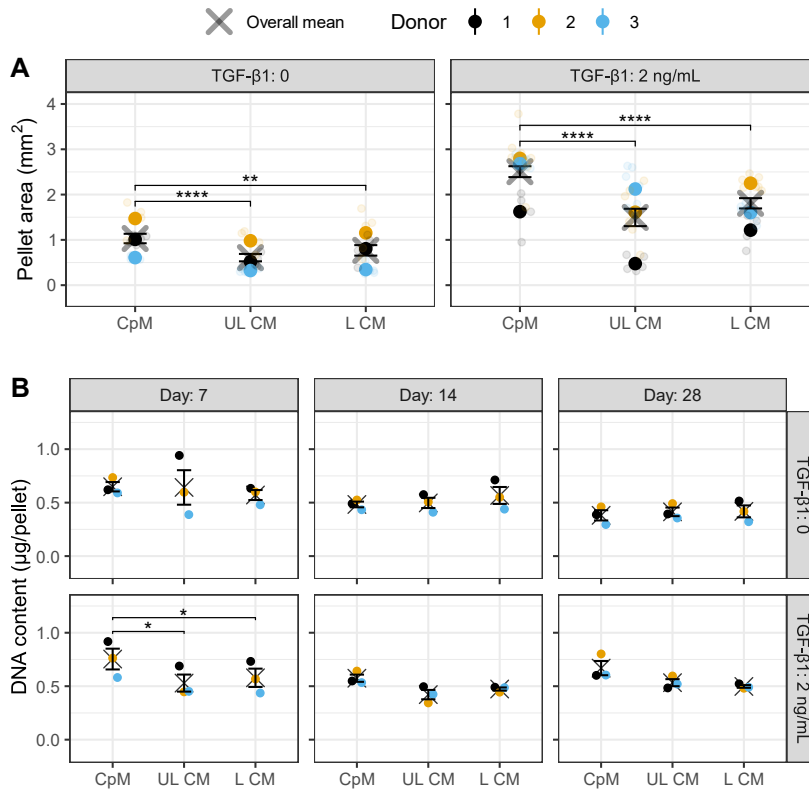
Fig. 4. (A) Pellet area of MSC pellets after 28 days of culture. Small transparent dots show single data points. (B) DNA content per pellet of MSCs after 7, 14, and 28 days of culture. Data from 3 donors. CpM: chondropermissive medium; UL CM: conditioned medium of unloaded samples; L CM: conditioned medium of loaded samples. Media either without (0) or with (2 ng/mL) TGF-β1. Error bars show SEM. *$p < .05$, **$p < .01$, ****$p < .0001$.

(CpM-: 29.93 µg/µg±5.25; UL CM-: 97.17 µg/µg±8.27; L CM-: 90.73 µg/µg±13.03 – CpM-vs. UL CM-: $p < .01$, CpM-vs. L CM-: $p < .01$.

CpM+: 40.15 µg/µg±9.81; UL CM+: 86.92 µg/µg±6.58; L CM+:97.58 µg/µg±8.14 – CpM + vs. UL CM+: $p < .01$, CpM + vs. L CM+: $p < .001$ – Fig. 7).

Within Cho pellets, L CM resulted in the highest sGAG content on day 14 in the absence of exogenous TGF-β1 (CpM-: 5.98 µg/µg ±0.68; UL CM-: 6.43 µg/µg±0.69; L CM-:13.26 µg/µg±0.44 – CpM-vs. UL CM-: $p < .001$, UL CM-vs. L CM-: $p < .001$) and with 2 ng/mL TGF-β1 (CpM+: 9.61 µg/µg±0.64; UL CM+: 8.56 µg/µg±1.07; L CM+: 11.65 µg/µg±1.48 – UL CM + vs. L CM+: $p < .05$ – Fig. 8). Over the course of the experiment, sGAG content within the Cho pellets increased (day 7 vs. day 21).

Total sGAG content found in the CM of Cho pellets was significantly higher for UL CM- and L CM-compared to CpM-without TGF-β1 supplementation (CpM-: 5.46 µg/µg±0.41; UL CM-: 18.1 µg/µg±1.83; L CM-: 23.04 µg/µg±0.98 – CpM-vs. UL CM-: $p < .01$, CpM-vs. L CM-: $p < .001$, UL CM-vs. L CM-: $p < .05$) and with 2 ng/mL TGF-β1 supplementation (CpM-: 9.45 µg/µg±0.41; UL CM-: 20.97 µg/µg ±0.59; L CM-: 23.84 µg/µg±0.23 – CpM + vs. UL CM+: $p < .0001$, CpM + vs. L CM+: $p < .0001$, UL CM + vs. L CM+: $p < .05$ – Fig. 9).

sGAG content in CM was also significantly higher for L CM compared to UL CM, with and without TGF-β1 addition.

3.7. Effect of CM on sGAG deposition in MSC pellet

Safranin O Fast Green staining only showed positive staining for sGAG for MSCs with TGF-β1 supplementation (Supplementary Fig. 5). For Cho, no difference was apparent between either group (with and without TGF-β1, Supplementary Fig. 6).

3.8. Effect of CM on gene expression of pellets

For MSC pellets without TGF-β1, there was a trend towards highest *COL1A1* expression for L CM over the different time points (Fig. 10). For MSC pellets supplemented with 2 ng/mL TGF-β1, adding CM (UL CM+ and L CM+) significantly increased *COL1A1* expression for day 14 (CpM + vs. UL CM+: $p < .05$, CpM + vs. L CM+: $p < .05$), though no trend was apparent. *SOX9* expression was in general lower for UL CM than L CM, although not statistically significant. For TGF-β1 supplemented MSC pellets, *SOX9* and *RUNX2*
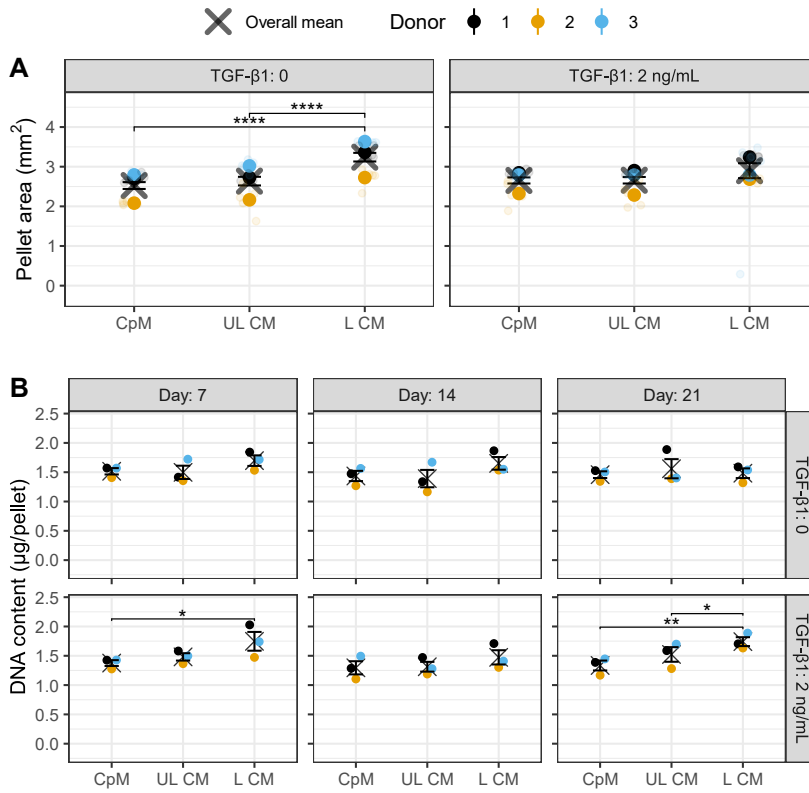
Fig. 5. (A) Pellet area of Cho pellets after 28 days of culture. Small transparent dots show single data points. (B) DNA content of Cho pellets after 7, 14, and 28 days of culture. Data from 3 donors. CpM: chondropermissive medium; UL CM: conditioned medium of unloaded samples; L CM: conditioned medium of loaded samples. Media either without (0) or with (2 ng/mL) TGF-β1. Error bars show SEM. Small transparent dots show single data points. *$p < .05$, **$p < .01$., ****$p < .0001$.
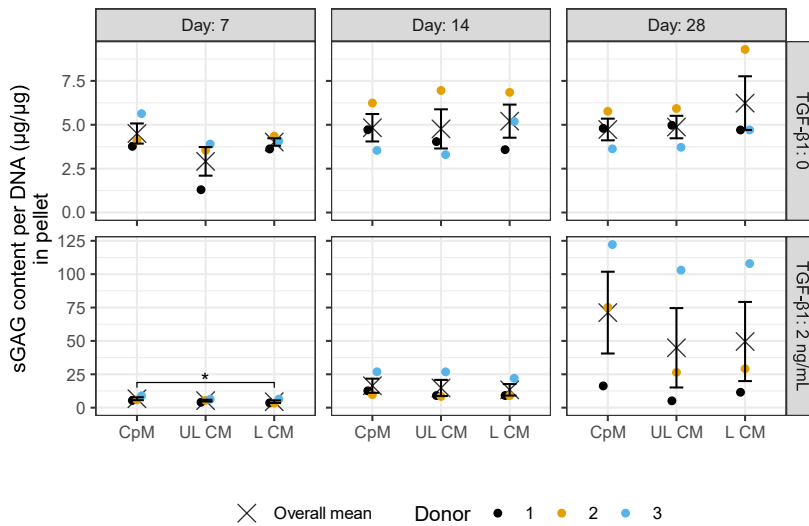

Fig. 6. sGAG content of MSC pellets after 7, 14, and 28 days of culture normalized to their respective DNA content. Data from 3 donors. CpM: chondropermissive medium; UL CM: conditioned medium of unloaded samples; L CM: conditioned medium of loaded samples. Media either without (0) or with (2 ng/mL) TGF-β1. Error bars show SEM. *$p < .05$.
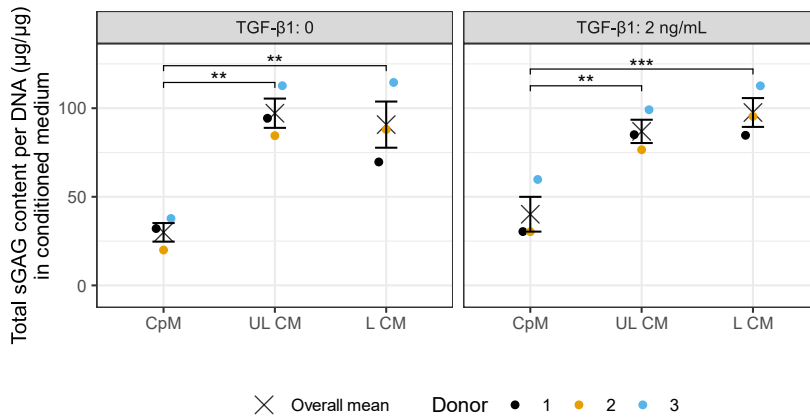
Fig. 7. Total sGAG content secreted by MSC pellets after 28 days of culture normalized to their respective DNA content. Data from 3 donors. CpM: chondropermissive medium; UL CM: conditioned medium of unloaded samples; L CM: conditioned medium of loaded samples. Media either without (0) or with (2 ng/mL) TGF-β1. Error bars show SEM. **$p < .01$, ***$p < .001$.
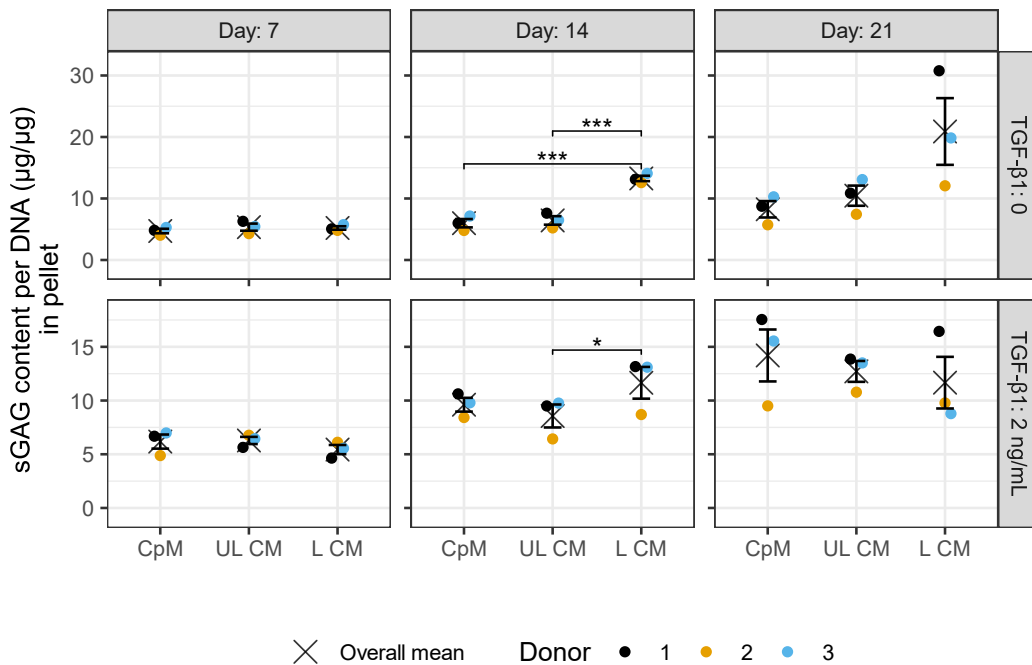

Fig. 8. sGAG content of Cho pellets after 7, 14, and 21 days of culture normalized to their respective DNA content. Data from 3 donors. CpM: chondropermissive medium; UL CM: conditioned medium of unloaded samples; L CM: conditioned medium of loaded samples. Media either without (0) or with (2 ng/mL) TGF-β1. Error bars show SEM. *$p < .05$, ***$p < .001$.

expression in UL CM+ was significantly lower than in CpM + on day 28 (CpM + vs. UL CM+: $p < .05$). MSC pellets without exogenous TGF-β1 showed a clear trend towards higher *MMP13* expression for CM-samples vs. CpM-, culminating with the highest fold change for L CM-at day 28, which was significantly higher than UL CM- and CpM-for the same time point (CpM-vs. L CM-: $p < .01$, UL CM-vs. L CM-: $p < .05$).

More differences were seen in different conditions without TGF-β1 for *COL2A1*, *COL10A1* and *ACAN* (Supplementary Fig. 3). For TGF-β1-free conditions, *COL2A1*, *ACAN* and *COL10A1*, gene expression was the highest for all time points for groups with L CM.

No trends were apparent for TGF-β1 supplemented MSC pellets for *COL2A1*, *COL10A1*, and *ACAN*.

For Cho pellets supplemented with 2 ng/mL TGF-β1, *COL1A1* was significantly lower for L CM + compared to both CpM+ and UL CM + on day 14 (CpM + vs. L CM+: $p < .05$, UL CM + vs. L CM+: $p.05$ – Fig. 11). For *COL10A1*, L CM-was significantly higher than
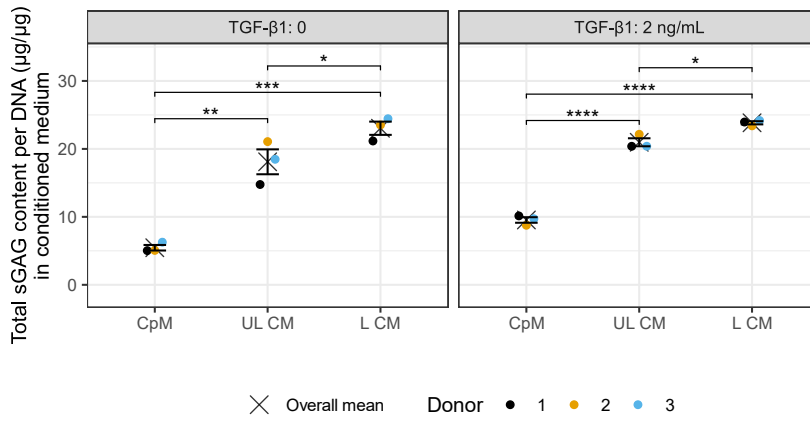
Fig. 9. Total sGAG content secreted by Cho pellets after 21 days of culture normalized to their respective DNA content. Data from 3 donors. CpM: chondropermissive medium; UL CM: conditioned medium of unloaded samples; L CM: conditioned medium of loaded samples. Media either without (0) or with (2 ng/mL) TGF-β1. Error bars show SEM. *$p < .05$, **$p < .01$, ***$p < .001$, ****$p < .0001$.
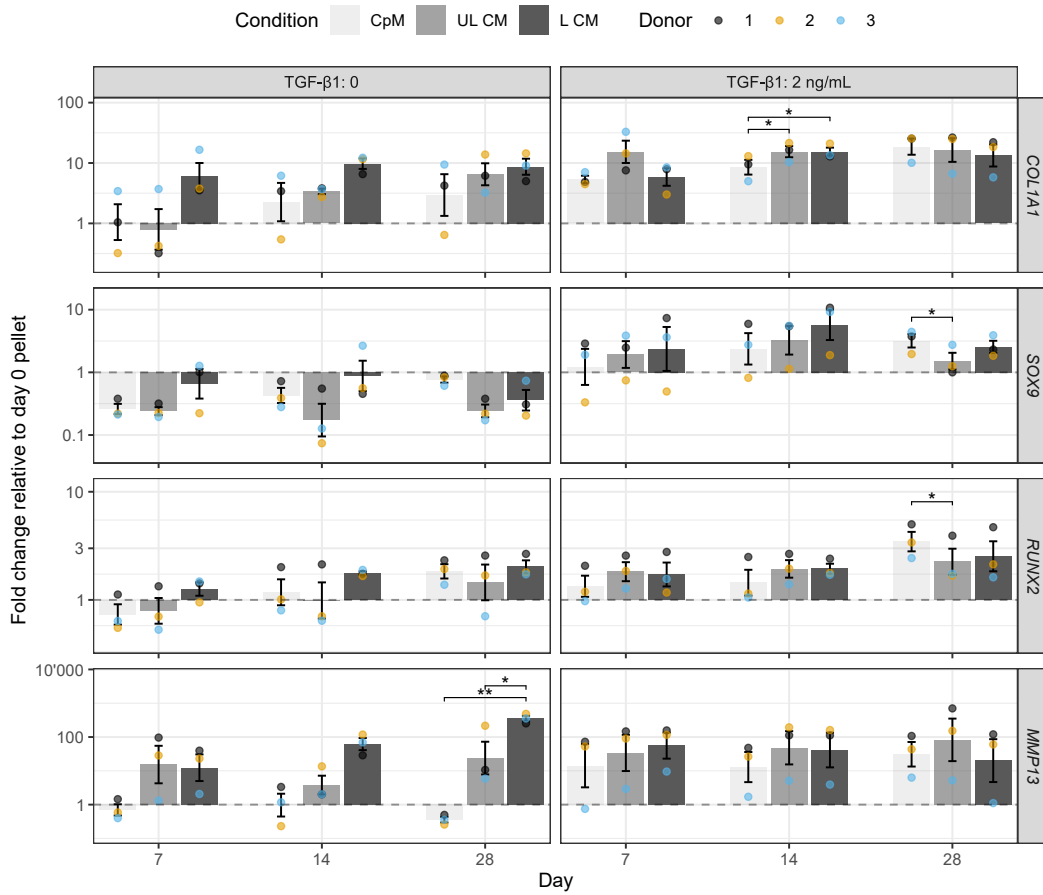

Fig. 10. PCR data of MSC pellets after 7, 14, and 28 days of culture. Data from 3 donors. CpM: chondropermissive medium; UL CM: conditioned medium of unloaded samples; L CM: conditioned medium of loaded samples. Media either without (0) or with (2 ng/mL) TGF-β1. *$p < .05$, **$p < .01$.

CpM- and UL CM-on day 14 without TGF-β1 (CpM-vs. L CM-: $p < .05$, UL CM-vs. L CM-: $p < .05$), whereas with TGF-β1 supplementation, the expression was significantly lower on day 14 for L CM + compared to CpM+ (CpM + vs. L CM+: $p < .05$). *ACAN* expression was significantly higher for L CM + compared to CpM + on day 7 for TGF-β1 supplemented samples (CpM + vs. L CM+: $p < .05$). L CM– resulted in a significantly higher *MMP13* expression compared to CpM- and UL CM-on day 21 without TGF-β1 addition (CpM-vs. L CM-: $p < .001$, UL CM-vs. L CM-: $p < .001$). *VCAN* expression was significantly higher in TGF-β1 supplemented samples on day 14 for L CM + compared to UL CM+ ($p < .05$) and day 21 for L CM + compared to CpM+ ($p < .05$).

For Cho pellets without TGF-β1 supplementation, *COL2A1* expression appeared to increase from CpM-to UL CM-to L CM-(Supplementary Fig. 4). This was not exactly the case for the samples with TGF-β1 addition, however, L CM + appeared to result in the highest expression. The values for *IL6* appeared to be the lowest for L CM, irrespective of TGF-β1 supplementation.

3.9. CM from loaded samples decreases T cell proliferation

Exposure of activated T cells to L CM from week 2 (L_w2) significantly decreased the division index compared to UL CM (UL_w2 – $p < .05$– Fig. 12). TGF-β1 immunoprecipitation did not affect this result.

4. Discussion

MSC secretome can be used to exert therapeutic effects, including immunomodulation and differentiation [17–20,44]. However, the exact mechanism and the responsible factors remain unclear. It is known that factors such as inflammation can affect secretion, thus we hypothesize mechanical loading of MSCs to play a role as well [45]. We previously showed our bioreactor system mechanically activated TGF-β1, a key protein in driving MSC chondrogenesis [14]. Additional factors affecting chondrogenesis, angiogenesis or immunomodulation were also detected using a small protein microarray [16]. It is therefore highly likely that many other soluble proteins within the CM are differentially expressed when exposing MSCs to mechanical stimulation.

The main aim of the study was to address changes observed in secretome driven by the MSCs response to of joint-mimicking multiaxial load alone. An additional group containing exogenous TGF-β1 was added to assess whether the presence of active TGF led to a modified response. As we have previously shown that 10 ng/mL exogenous TGF- β1 interfered with MSC response to load, we used a lower dose of 2 ng/mL, which still leads to chondrogenesis as seen in the data presented here. After analyzing the CM using a 2000 protein array, we investigated the effect of the CM on MSC and Cho chondrogenic behavior, and on cells from joint-associated tissues, namely T cells.

While most of the proteins could be detected in the CM of both L and UL MSCs, PCA clearly showed differences between both groups (Fig. 3). The first principal component separated the samples by load, the second component separated between day 0 samples (1 day exposure to cells) and CM that had been in contact with cells for more than 1 day (pooled CM from week 2, 3 and 4). Additionally, SAM revealed 179 protein targets that were significantly different when comparing L CM vs. UL CM (Supplementary Tables 7–1).

In the only other similar study, we conducted a shorter-term experiment within a bioreactor and compared UL CM with L CM [16]. There, L CM showed significantly higher abundance of various proteins, such as activated leukocyte cell adhesion molecule (ALCAM), c-c motif chemokine ligand 7 and 20 (CCL7 and CCL20), c-x-c motif chemokine ligand 13 (CXCL13), macrophage migration inhibitory factor (MIF), MMP13 and vascular endothelial growth factor A (VEGFA) compared to UL CM on day eight of culture. The inverse was the case for CXCL1, CXCL2 and CXCL3. The present study showed comparable trends, but SAM revealed only significant differences for CXCL13, CXCL1, MMP13 and VEGFA (Supplementary Fig. 1). Non-significance could however be attributed to the fact that we used a different analysis method with pooled CM from different weekly time points. In fact, our array data shows that the abundance for various proteins can vary bi-directionally among the different weekly pooled samples.

Only L CM (and day 0 CM) showed integrin β-6 secretion (Supplementary Fig. 1)., indicative of TGF-β1 activation via matrix-latent TGF-β complex interactions [46–48]. Interestingly, integrin β-6 was also increased at day 0, possibly due to cellular stress during scaffold seeding, such as trypsinization. This integrin is upregulated in conditions like lung injury [49] and is linked to increased αV integrin expression, forming a complex regulatory cycle [50].

As expected from previous experiments [25], loaded samples showed higher amounts of sGAG within the constructs, while less sGAG was detected in the CM (Fig. 2). We hypothesize that a negative feedback loop decreases sGAG production if there is sufficient amount of sGAG within the pericellular matrix.

Addition of exogenous TGF-β1 during *in vitro* chondrogenesis is considered to be the gold standard to assess chondrogenic potential of MSCs. However, the classically used dose of 10 ng/mL is supraphysiological and has been shown to be a powerful stimulus that masks synergistic effects, such as mechanical stimulation [14]. To increase the potential to identify relevant effects of secretome on cell phenotype, we reduced the dose to be closer to physiological conditions [51].

TGF-β1 supplementation of MSC pellets has been shown to increase the size of the pellet by increasing the pericellular matrix [52]. We observed an increase in pellet area in MSCs exposed to TGF-β1 (Fig. 4). Conversely, no such effect was visible for Cho (Fig. 5). In general, the area of MSC pellets was significantly decreased for samples subjected to CM, as opposed to CpM. This was the case with and without TGF-β1 supplementation. On the other hand, in TGF-β1-free Cho pellets, L CM significantly increased the pellet area, compared to both UL CM and CpM (Fig. 5). This indicates that the influence of CM on chondrogenesis is different from its effect on chondrogenic maintenance.

Interestingly, UL and L CM decreased DNA content in TGF-β1 supplemented MSC pellets after 7 days compared to CpM (Fig. 4). For the remaining groups and time points, the DNA content appeared quite stable. We expected an increase in DNA content for TGF-β1 supplemented MSC pellets, as seen in a study by Futrega et al. [52]. However, another study has shown that there is little effect from
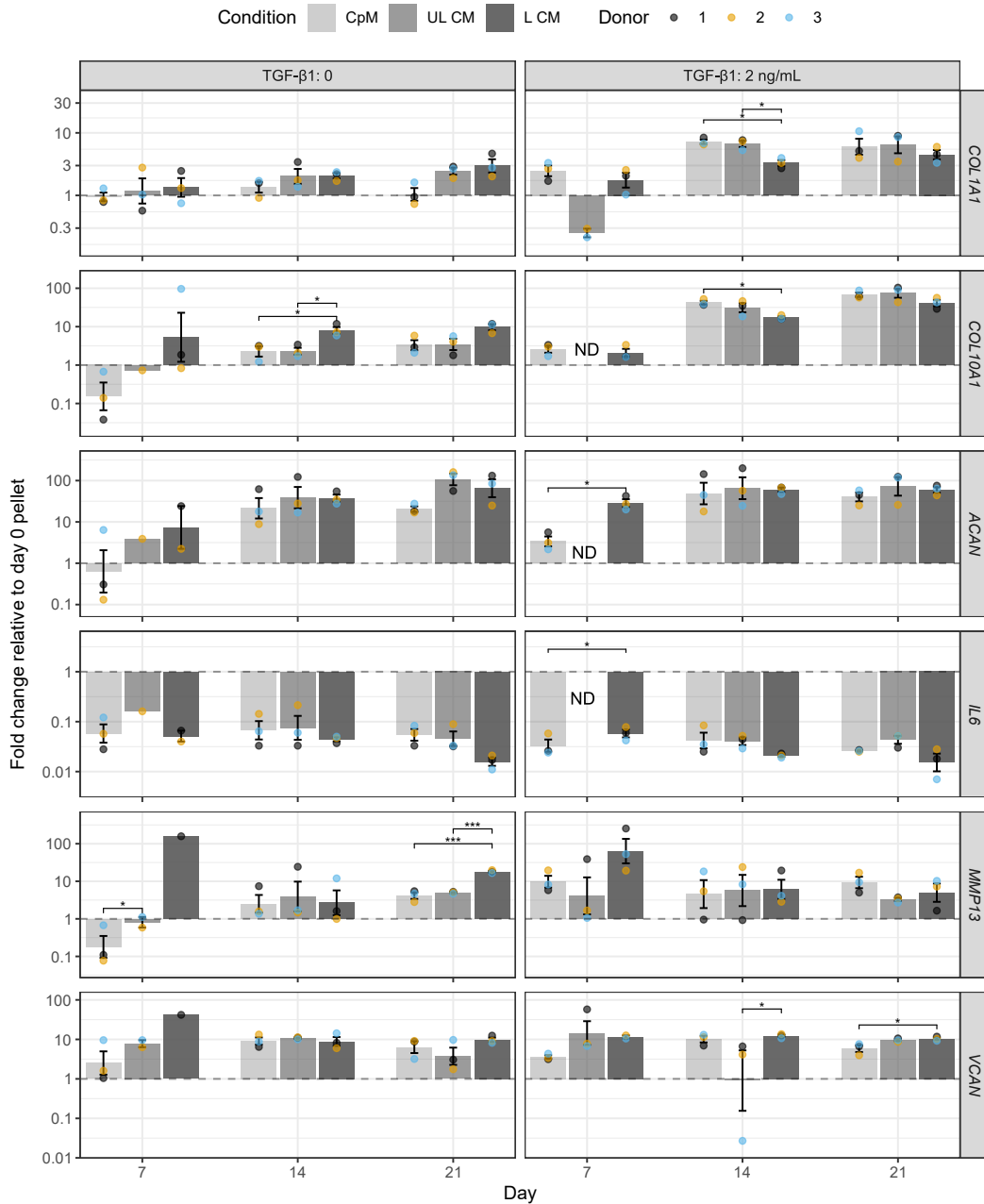
Fig. 11. PCR data of Cho pellets after 7, 14, and 21 days of culture. CpM: chondropermissive medium; UL CM: conditioned medium of unloaded samples; L CM: conditioned medium of loaded samples. Media either without (0) or with (2 ng/mL) TGF-β1. ND = Not Detected. Error bars show SEM. *$p < .05$, ***$p < .001$.

supplementation of another TGF-β isoform on DNA content over time [53]. The DNA content of Cho pellets remained unaffected if not supplemented with TGF-β1. However, the addition of 2 ng/mL TGF-β1 to L CM showed a synergistic effect at day 21 (Fig. 5).

Unsurprisingly, exogenous TGF-β1 dramatically increased MSC pellet sGAG content by D28 compared to TGF-β1 free samples at the same time point ($p < .05$), as previously shown [52]. For Cho, sGAG retention increased for L CM, with and without TGF-β1 supplementation at day 14, suggesting a constituent within L CM is able to increase matrix deposition (Fig. 8).

sGAG secreted into the CM of both MSC (Fig. 7) and Cho pellets (Fig. 9) was significantly higher for UL CM and L CM when compared to CpM alone ($p < .01$ or greater). This is potentially due to the sGAG that was already present in the CM added to the CpM in 1:1. The highest sGAG amount would have been expected for UL CM, as more sGAG was detected in CM from the scaffolds that were not loaded. Yet, more sGAG was detected in media conditioned by MSC and Cho pellets exposed to L CM (Figs. 7 and 9), indicative of
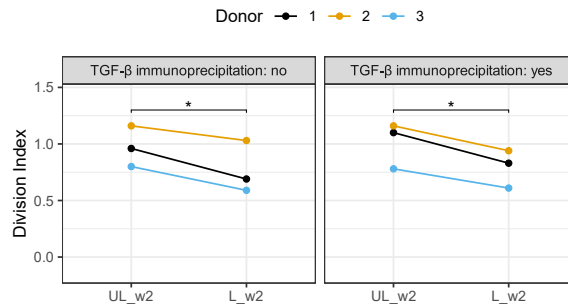
Fig. 12. Division index of T cells after activation with and without TGF-β immunoprecipitation. Exposure to pooled conditioned medium from week 2 to unloaded samples (UL_w) and loaded samples (L_w2). *$p < .05$.

increased production in cells exposed to L CM.

In the absence of TGF-β1 supplementation, expression of *MMP13* in MSC pellets was low. Exposure to L CM significantly increased *MMP13* expression by day 28 (Fig. 10). Additionally, TGF-β1 supplementation alone increased *MMP13* expression, resulting in no effect on expression due to load. Similarly, Cho in the absence of TGF-β1 with L CM led to a significant increase in *MMP1*3 by 21 days (Fig. 11). MMP13 is typically involved in ECM remodeling and is widely associated with hypertrophic differentiation often in the context of MSC [54], which suggests an unstable chondrogenesis. Furthermore, In the absence of TGF-β1, L CM led to an increase in *COL10A1* expression on day 14. Conversely, the addition of 2 ng/mL TGF-β1 led to decreased *COL10A1* expression in the L CM group at the same time point.

In summary, TGF-β1-free L CM appeared to lead to a trend towards strongest chondrogenic phenotype for both MSC and Cho. However, the chondrogenic gene expression in TGF-β1-free L CM-was not strong enough for it to be reflected in histology.

To investigate the effect of the MSC secretome on the immune system, a T cell proliferation experiment was performed, as T cells have been shown to be suppressed by TGF-β1 [55,56]. Moreover, it has been shown that exposing MSCs to pro-inflammatory cytokines such as interleukin 1 beta (IL-1β) and tumor necrosis factor (TNF-α) generates a T cell proliferation-suppressive secretome [57]. Since L CM showed increases in pro-inflammatory cytokines IL-1β and TNF-α, we investigated whether joint-mimicking mechanical loading was sufficient to elicit a similar response [58]. In our experiment, activated T cells that were exposed to L CM from week 2 decreased their division index (Fig. 12). However, TGF-β immunoprecipitation did not restore the reduced division index, thus, this effect is not directly mediated by TGF-β. Protectin (*CD59*) could play a role in this process, as protectin has been shown to downregulate T cell activity in vivo [59] and L CM showed a higher abundance of CD59 compared to UL CM (Supplementary Fig. 1). Another factor that has been reported to have T-cell-suppressive function is Charcot-Leyden crystal galectin (CLC) [60]. SAM showed that this factor was significantly more abundant in L CM and UL CM (Supplementary Fig. 1).

In this follow-up study to Gardner et al. [16], we examined how mechanical stimulation affects MSC secretory function, rather than its direct impact on MSC chondrogenesis. Understanding these effects could reveal how MSC secretome influences progenitor cell differentiation, immune regulation, and cartilage healing. Insights into the chondro-regenerative potential of mechanically loaded MSC secretome could lead to the development of off-the-shelf, acellular therapeutic products with advantages in storage, handling, and shelf-life [61].

Overall, conditioned media decreased MSC DNA content and pellet size, while increasing sGAG release into the media. Conversely, L CM increased Cho pellet size and, in the presence of exogenous TGF-β1, increased DNA content. L CM also increased sGAG/DNA and secreted sGAG in Cho pellets. This would indicate that the secretome of mechanically loaded MSCs may be more beneficial in inducing a repair response in resident chondrocytes, rather than enhancing direct MSC chondrogenesis. The additional benefit of reducing T cell activation may further improve healing by reducing local inflammation.

Our data underscore the secretome's potential and complexity. *In vitro* models like ours isolate the secretome from the complex in vivo environment to study mechanical stimulation effects. Future research will focus on concentrating the secretome and exploring other joint-related processes, such as angiogenesis. Understanding how mechanical loading modulates the secretome could inform treatment strategies for traumatic cartilage injuries, potentially reducing the health costs associated with post-traumatic osteoarthritis.

5. Limitations of the study

This study has certain limitations, such as the sample size, which is especially problematic in very heterogeneous cell populations such as MSCs [62,63]. The donors might react differently to any stimulus, which impedes detection of significant trends with standard statistical approaches. Also, magnitude of change does not always coincide with biological relevance and therefore, setting the fold change limit at 2 for the SAM might have obfuscated potentially relevant effects [64]. The CM was pooled from different donors and time points to obtain a larger volume and to reduce treatment groups. However, this might have masked donor-specific and time-specific effects. We supplemented the CM 1:1 with CpM to refresh the final CM with nutrients that had been depleted during MSC culture within the scaffolds. Consequently, the effect of the secretome might have been diluted even further. Perhaps, concentrating

the CM before diluting would have been an option, as was shown by Chen et al. [65] Trends towards chondrogenesis were apparent in both gene and protein expression. However, the findings did not translate into histology, potentially due to the low concentration of the secreted proteins and the poor retention of matrix products by fibrin. Finally, this microarray only shows the secretion of 2000 pre-selected targets and not all possible targets and the proteins only reflect a small part of the entire secretome, which also contains lipids, nucleic acids and extracellular vesicles that exert their own effects [66]. Another weakness of this study is that the ethics permission does not provide information on possible comorbidities (*e.g.* osteoarthritis) of the MSC donors, which could affect the results.

CRediT authorship contribution statement

Yann D. Ladner: Writing – review & editing, Writing – original draft, Investigation, Formal analysis, Data curation, Conceptualization. **Ursula Menzel:** Writing – review & editing, Methodology, Investigation, Formal analysis, Data curation. **Keith Thompson:** Writing – review & editing, Writing – original draft, Project administration, Investigation, Formal analysis, Data curation, Conceptualization. **Angela R. Armiento:** Writing – review & editing, Writing – original draft, Supervision, Project administration, Investigation, Formal analysis, Data curation, Conceptualization. **Martin J. Stoddart:** Writing – review & editing, Writing – original draft, Supervision, Project administration, Funding acquisition, Formal analysis, Data curation, Conceptualization.

Data availability statement

Data will be made available on request.

Funding

Declaration of competing interest

The authors declare the following financial interests/personal relationships which may be considered as potential competing interests:Martin Stoddart reports financial support was provided by Swiss National Science Foundation. Martin Stoddart reports a relationship with TERMIS EU that includes: board membership. If there are other authors, they declare that they have no known competing financial interests or personal relationships that could have appeared to influence the work reported in this paper.

Acknowledgments

Appendix A. Supplementary data

Supplementary data to this article can be found online at https://doi.org/10.1016/j.heliyon.2025.e42234.

References

[1] T.D. Brown, R.C. Johnston, C.L. Saltzman, J.L. Marsh, J.A. Buckwalter, Posttraumatic osteoarthritis: a first estimate of incidence, prevalence, and burden of disease, J. Orthop. Trauma 20 (2006) 739–744, https://doi.org/10.1097/01.bot.0000246468.80635.ef.
[2] A.C. Thomas, T. Hubbard-Turner, E.A. Wikstrom, R.M. Palmieri-Smith, Epidemiology of posttraumatic osteoarthritis, J. Athl. Train. 52 (2017) 491–496, https://doi.org/10.4085/1062-6050-51.5.08.
[3] E.V. Medvedeva, E.A. Grebenik, S.N. Gornostaeva, V.I. Telpuhov, A.V. Lychagin, P.S. Timashev, A.S. Chagin, Repair of damaged articular cartilage: current approaches and future directions, Int. J. Mol. Sci. 19 (2018), https://doi.org/10.3390/ijms19082366.
[4] J.R. Steadman, W.G. Rodkey, J.J. Rodrigo, Microfracture: surgical technique and rehabilitation to treat chondral defects, Clin. Orthop. Relat. Res. S362–369 (2001), https://doi.org/10.1097/00003086-200110001-00033.
[5] A.J. Vernengo, M. Alini, A.R. Armiento, Cartilage tissue engineering, in: Tissue Engineering Using Ceramics and Polymers, 2022, pp. 555–586, https://doi.org/10.1016/b978-0-12-820508-2.00004-0.
[6] A.R. Armiento, M. Alini, M.J. Stoddart, Articular fibrocartilage - why does hyaline cartilage fail to repair? Adv. Drug Deliv. Rev. 146 (2019) 289–305, https://doi.org/10.1016/j.addr.2018.12.015.
[7] D. Goyal, A. Goyal, S. Keyhani, E.H. Lee, J.H. Hui, Evidence-based status of second- and third-generation autologous chondrocyte implantation over first generation: a systematic review of level I and II studies, Arthroscopy 29 (2013) 1872–1878, https://doi.org/10.1016/j.arthro.2013.07.271.
[8] Y. Nam, Y.A. Rim, J. Lee, J.H. Ju, Current therapeutic strategies for stem cell-based cartilage regeneration, Stem Cell. Int. 2018 (2018) 1–20, https://doi.org/10.1155/2018/8490489.
[9] P. Orth, L. Gao, H. Madry, Microfracture for cartilage repair in the knee: a systematic review of the contemporary literature, Knee Surg. Sports Traumatol. Arthrosc. 28 (2020) 670–706, https://doi.org/10.1007/s00167-019-05359-9.
[10] J.P. Benthien, P. Behrens, Autologous matrix-induced chondrogenesis (AMIC): combining microfracturing and a collagen I/III matrix for articular cartilage resurfacing, Cartilage 1 (2010) 65–68, https://doi.org/10.1177/1947603509360044.

[11] C.R. Lee, S. Grad, K. Gorna, S. Gogolewski, A. Goessl, M. Alini, Fibrin-polyurethane composites for articular cartilage tissue engineering: a preliminary analysis, Tissue Eng. 11 (2005) 1562–1573, https://doi.org/10.1089/ten.2005.11.1562.

[12] O.F.W. Gardner, G. Musumeci, A.J. Neumann, D. Eglin, C.W. Archer, M. Alini, M.J. Stoddart, Asymmetrical seeding of MSCs into fibrin-poly(ester-urethane) scaffolds and its effect on mechanically induced chondrogenesis, Journal of tissue engineering and regenerative medicine 11 (2017) 2912–2921, https://doi.org/10.1002/term.2194.

[13] O. Schatti, S. Grad, J. Goldhahn, G. Salzmann, Z. Li, M. Alini, M.J. Stoddart, A combination of shear and dynamic compression leads to mechanically induced chondrogenesis of human mesenchymal stem cells, Eur. Cell. Mater. 22 (2011) 214–225, https://doi.org/10.22203/ecm.v022a17.

[14] Z. Li, L. Kupcsik, S.J. Yao, M. Alini, M.J. Stoddart, Mechanical load modulates chondrogenesis of human mesenchymal stem cells through the TGF-beta pathway, J. Cell Mol. Med. 14 (2010) 1338–1346, https://doi.org/10.1111/j.1582-4934.2009.00780.x.

[15] B. Johnstone, T.M. Hering, A.I. Caplan, V.M. Goldberg, J.U. Yoo, In vitro chondrogenesis of bone marrow-derived mesenchymal progenitor cells, Exp. Cell Res. 238 (1998) 265–272, https://doi.org/10.1006/excr.1997.3858.

[16] O.F. Gardner, N. Fahy, M. Alini, M.J. Stoddart, Differences in human mesenchymal stem cell secretomes during chondrogenic induction, Eur. Cell. Mater. 31 (2016) 221–235, https://doi.org/10.22203/ecm.v031a15.

[17] P.K. L, S. Kandoi, R. Misra, V. S, R. K, R.S. Verma, The mesenchymal stem cell secretome: a new paradigm towards cell-free therapeutic mode in regenerative medicine, Cytokine Growth Factor Rev. 46 (2019) 1–9, https://doi.org/10.1016/j.cytogfr.2019.04.002.

[18] N. Alessio, S. Özcan, K. Tatsumi, A. Murat, G. Peluso, M. Dezawa, U. Galderisi, The secretome of MUSE cells contains factors that may play a role in regulation of stemness, apoptosis and immunomodulation, Cell Cycle 16 (2017) 33–44, https://doi.org/10.1080/15384101.2016.1211215.

[19] K. Kološa, H. Motaln, C. Herold-Mende, M. Koršič, T.T. Lah, Paracrine effects of mesenchymal stem cells induce senescence and differentiation of glioblastoma stem-like cells, Cell Transplant. 24 (2015) 631–644, https://doi.org/10.3727/096368915x687787.

[20] M.E. Cooke, A.A. Allon, T. Cheng, A.C. Kuo, H.T. Kim, T.P. Vail, R.S. Marcucio, R.A. Schneider, J.C. Lotz, T. Alliston, Structured three-dimensional co-culture of mesenchymal stem cells with chondrocytes promotes chondrogenic differentiation without hypertrophy, Osteoarthritis Cartilage 19 (2011) 1210–1218, https://doi.org/10.1016/j.joca.2011.07.005.

[21] T.S. de Windt, L.A. Vonk, I.C. Slaper-Cortenbach, M.P. van den Broek, R. Nizak, M.H. van Rijen, R.A. de Weger, W.J. Dhert, D.B. Saris, Allogeneic mesenchymal stem cells stimulate cartilage regeneration and are Safe for single-stage cartilage repair in humans upon mixture with recycled autologous chondrons, Stem Cell. 35 (2017) 256–264, https://doi.org/10.1002/stem.2475.

[22] E. Bari, I. Ferrarotti, M.L. Torre, A.G. Corsico, S. Perteghella, Mesenchymal stem/stromal cell secretome for lung regeneration: the long way through "pharmaceuticalization" for the best formulation, J. Contr. Release 309 (2019) 11–24, https://doi.org/10.1016/j.jconrel.2019.07.022.

[23] E. Bari, S. Perteghella, D. Di Silvestre, M. Sorlini, L. Catenacci, M. Sorrenti, G. Marrubini, R. Rossi, G. Tripodo, P. Mauri, et al., Pilot production of mesenchymal stem/stromal freeze-dried secretome for cell-free regenerative nanomedicine: a validated GMP-compliant process, Cells 7 (2018) 190, https://doi.org/10.3390/cells7110190.

[24] H.A. Owida, T. De Las Heras Ruiz, A. Dhillon, Y. Yang, N.J. Kuiper, Co-culture of chondrons and mesenchymal stromal cells reduces the loss of collagen VI and improves extracellular matrix production, Histochem. Cell Biol. 148 (2017) 625–638, https://doi.org/10.1007/s00418-017-1602-4.

[25] Y.D. Ladner, H. Kasper, A.R. Armiento, M.J. Stoddart, A multi-well bioreactor for cartilage tissue engineering experiments, iScience 26 (2023), https://doi.org/10.1016/j.isci.2023.107092.

[26] L.I. Sakkas, C.D. Platsoucas, The role of T cells in the pathogenesis of osteoarthritis, Arthritis Rheum. 56 (2007) 409–424, https://doi.org/10.1002/art.22369.

[27] A.R. Armiento, Y.D. Ladner, E. Della Bella, M.J. Stoddart, Isolation and in vitro chondrogenic differentiation of human bone marrow-derived mesenchymal stromal cells, in: M.J. Stoddart, E. Della Bella, A.R. Armiento (Eds.), Cartilage Tissue Engineering, Springer US, 2023, pp. 65–73, https://doi.org/10.1007/978-1-0716-2839-3_6.

[28] Z. Li, L. Kupcsik, S.J. Yao, M. Alini, M.J. Stoddart, Chondrogenesis of human bone marrow mesenchymal stem cells in fibrin-polyurethane composites, Tissue Eng. 15 (2009) 1729–1737, https://doi.org/10.1089/ten.tea.2008.0247.

[29] S. Francioli, C. Cavallo, B. Grigolo, I. Martin, A. Barbero, Engineered cartilage maturation regulates cytokine production and interleukin-1beta response, Clin. Orthop. Relat. Res. 469 (2011) 2773–2784, https://doi.org/10.1007/s11999-011-1826-x.

[30] W. Chang, J. Cheng, J.J. Allaire, C. Sievert, B. Schloerke, Y. Xie, J. Allen, J. McPherson, A. Dipert, B. Borges, Shiny: Web Application Framework for R, 2023.

[31] FlowJo's Proliferation platform. https://docs.flowjo.com/flowjo/experiment-based-platforms/proliferation/.

[32] Y.D. Ladner, M. Alini, A.R. Armiento, The dimethylmethylene blue assay (DMMB) for the quantification of sulfated glycosaminoglycans, in: M.J. Stoddart, E. Della Bella, A.R. Armiento (Eds.), Cartilage Tissue Engineering, Springer US, 2023, pp. 115–121, https://doi.org/10.1007/978-1-0716-2839-3_9.

[33] Sigma TRI Reagent® Protocol. https://www.sigmaaldrich.com/CH/en/technical-documents/protocol/protein-biology/protein-lysis-and-extraction/tri-reagent.

[34] K.J. Livak, T.D. Schmittgen, Analysis of relative gene expression data using real-time quantitative PCR and the 2(-Delta Delta C(T)) Method, Methods 25 (2001) 402–408, https://doi.org/10.1006/meth.2001.1262.

[35] J. Schindelin, I. Arganda-Carreras, E. Frise, V. Kaynig, M. Longair, T. Pietzsch, S. Preibisch, C. Rueden, S. Saalfeld, B. Schmid, et al., Fiji: an open-source platform for biological-image analysis, Nat. Methods 9 (2012) 676–682, https://doi.org/10.1038/nmeth.2019.

[36] t. Posit, RStudio: Integrated Development Environment for R, 2023.

[37] R.C. Team, R: A Language and Environment for Statistical Computing, 2023.

[38] K. Blighe, A. Lun, PCAtools: PCAtools: Everything Principal Components Analysis, 2023, https://doi.org/10.18129/B9.bioc.PCAtools.

[39] L. Yan, Ggvenn: Draw Venn Diagram by 'ggplot2', 2023.

[40] R. Tibshirani, M.J. Seo, G. Chu, B. Narasimhan, J. Li, Samr: SAM: Significance Analysis of Microarrays, 2018.

[41] A. Kuznetsova, P.B. Brockhoff, R.H.B. Christensen, lmerTest package: tests in linear mixed effects models, J. Stat. Software 82 (2017) 1–26, https://doi.org/10.18637/jss.v082.i13.

[42] D. Bates, M. Mächler, B. Bolker, S. Walker, Fitting linear mixed-effects models using lme4, J. Stat. Software 67 (2015) 1–48, https://doi.org/10.18637/jss.v067.i01.

[43] R.V. Lenth, Emmeans: Estimated Marginal Means, Aka Least-Squares Means, 2023.

[44] R. Estrada, N. Li, H. Sarojini, J. An, M.-J. Lee, E. Wang, Secretome from mesenchymal stem cells induces angiogenesis via Cyr61, J. Cell. Physiol. 219 (2009) 563–571, https://doi.org/10.1002/jcp.21701.

[45] E. Ragni, C. Perucca Orfei, P. De Luca, C. Mondadori, M. Viganò, A. Colombini, L. De Girolamo, Inflammatory priming enhances mesenchymal stromal cell secretome potential as a clinical product for regenerative medicine approaches through secreted factors and EV-miRNAs: the example of joint disease, Stem Cell Res. Ther. 11 (2020), https://doi.org/10.1186/s13287-020-01677-9.

[46] J.S. Munger, X. Huang, H. Kawakatsu, M.J.D. Griffiths, S.L. Dalton, J. Wu, J.-F. Pittet, N. Kaminski, C. Garat, M.A. Matthay, et al., A mechanism for regulating pulmonary inflammation and fibrosis: the integrin αvβ6 binds and activates latent TGF β1, Cell 96 (1999) 319–328, https://doi.org/10.1016/s0092-8674(00)80545-0.

[47] P.J. Wipff, B. Hinz, Integrins and the activation of latent transforming growth factor beta1 - an intimate relationship, Eur. J. Cell Biol. 87 (2008) 601–615, https://doi.org/10.1016/j.ejcb.2008.01.012.

[48] J.P. Annes, Y. Chen, J.S. Munger, D.B. Rifkin, Integrin alphaVbeta6-mediated activation of latent TGF-beta requires the latent TGF-beta binding protein-1, J. Cell Biol. 165 (2004) 723–734, https://doi.org/10.1083/jcb.200312172.

[49] J.M. Breuss, J. Gallo, H.M. Delisser, I.V. Klimanskaya, H.G. Folkesson, J.F. Pittet, S.L. Nishimura, K. Aldape, D.V. Landers, W. Carpenter, et al., Expression of the β6 integrin subunit in development, neoplasia and tissue repair suggests a role in epithelial remodeling, J. Cell Sci. 108 (1995) 2241–2251, https://doi.org/10.1242/jcs.108.6.2241.

[50] F.A. Mamuya, M.K. Duncan, aV integrins and TGF-β-induced EMT: a circle of regulation, J. Cell Mol. Med. 16 (2012) 445–455, https://doi.org/10.1111/j.1582-4934.2011.01419.x.

[51] T. Wang, S. Dogru, Z. Dai, S.Y. Kim, N.A. Vickers, M.B. Albro, Physiologic Doses of TGF-Beta Improve the Composition of Engineered Articular Cartilage, bioRxiv, 2023, https://doi.org/10.1101/2023.09.27.559554.

[52] K. Futrega, P.G. Robey, T.J. Klein, R.W. Crawford, M.R. Doran, A single day of TGF-β1 exposure activates chondrogenic and hypertrophic differentiation pathways in bone marrow-derived stromal cells, Commun. Biol. 4 (2021), https://doi.org/10.1038/s42003-020-01520-0.

[53] H. Fan, C. Zhang, J. Li, L. Bi, L. Qin, H. Wu, Y. Hu, Gelatin microspheres containing TGF-β3 enhance the chondrogenesis of mesenchymal stem cells in modified pellet culture, Biomacromolecules 9 (2008) 927–934, https://doi.org/10.1021/bm7013203.

[54] M.B. Mueller, R.S. Tuan, Functional characterization of hypertrophy in chondrogenesis of human mesenchymal stem cells, Arthritis Rheum. 58 (2008) 1377–1388, https://doi.org/10.1002/art.23370.

[55] M. Di Nicola, C. Carlo-Stella, M. Magni, M. Milanesi, P.D. Longoni, P. Matteucci, S. Grisanti, A.M. Gianni, Human bone marrow stromal cells suppress T-lymphocyte proliferation induced by cellular or nonspecific mitogenic stimuli, Blood 99 (2002) 3838–3843, https://doi.org/10.1182/blood.v99.10.3838.

[56] J.H. Kehrl, L.M. Wakefield, A.B. Roberts, S. Jakowlew, M. Alvarez-Mon, R. Derynck, M.B. Sporn, A.S. Fauci, Production of transforming growth factor beta by human T lymphocytes and its potential role in the regulation of T cell growth, J. Exp. Med. 163 (1986) 1037–1050, https://doi.org/10.1084/jem.163.5.1037.

[57] M. Breitman, T.L. Bonfield, A.I. Caplan, H.M. Lazarus, M. Haghiac, S. Lasalvia, J. Reese-Koc, N.G. Singer, Optimization of human mesenchymal stem cells for rheumatoid arthritis: implications for improved therapeutic outcomes, ACR Open Rheumatology 4 (2022) 152–160, https://doi.org/10.1002/acr2.11356.

[58] P. Renner, E. Eggenhofer, A. Rosenauer, F.C. Popp, J.F. Steinmann, P. Slowik, E.K. Geissler, P. Piso, H.J. Schlitt, M.H. Dahlke, Mesenchymal stem cells require a sufficient, ongoing immune response to exert their immunosuppressive function, Transplant. Proc. 41 (2009) 2607–2611, https://doi.org/10.1016/j.transproceed.2009.06.119.

[59] B. Sivasankar, M.P. Longhi, K.M.E. Gallagher, G.J. Betts, B.P. Morgan, A.J. Godkin, A.M. Gallimore, CD59 blockade enhances antigen-specific CD4+ T cell responses in humans: a new target for cancer immunotherapy? J. Immunol. 182 (2009) 5203–5207, https://doi.org/10.4049/jimmunol.0804243.

[60] C. Lingblom, J. Andersson, K. Andersson, C. Wennerås, Regulatory eosinophils suppress T cells partly through galectin-10, J. Immunol. 198 (2017) 4672–4681, https://doi.org/10.4049/jimmunol.1601005.

[61] F.J. Vizoso, N. Eiro, S. Cid, J. Schneider, R. Perez-Fernandez, Mesenchymal stem cell secretome: toward cell-free therapeutic strategies in regenerative medicine, Int. J. Mol. Sci. 18 (2017), https://doi.org/10.3390/ijms18091852.

[62] M.J. Stoddart, R.G. Richards, M. Alini, In vitro experiments with primary mammalian cells: to pool or not to pool? Eur. Cell. Mater. 24 (2012) i–ii.

[63] M.F. Pittenger, D.E. Discher, B.M. Péault, D.G. Phinney, J.M. Hare, A.I. Caplan, Mesenchymal stem cell perspective: cell biology to clinical progress, NPJ Regen. Med. 4 (2019), https://doi.org/10.1038/s41536-019-0083-6.

[64] A.L. Tarca, R. Romero, S. Draghici, Analysis of microarray experiments of gene expression profiling, Am. J. Obstet. Gynecol. 195 (2006) 373–388, https://doi.org/10.1016/j.ajog.2006.07.001.

[65] Y.-C. Chen, Y.-W. Chang, K.P. Tan, Y.-S. Shen, Y.-H. Wang, C.-H. Chang, Can mesenchymal stem cells and their conditioned medium assist inflammatory chondrocytes recovery? PLoS One 13 (2018) e0205563 https://doi.org/10.1371/journal.pone.0205563.

[66] N. Li, J. Hua, Interactions between mesenchymal stem cells and the immune system, Cell. Mol. Life Sci. 74 (2017) 2345–2360, https://doi.org/10.1007/s00018-017-2473-5.